Development and Optimization of a Fluorescent Imaging System to Detect Amyloid-β Proteins: Phantom Study

David Tes[1], Karl Kratkiewicz[1], Ahmed Aber[2], Luke Horton[3],
Mohsin Zafar[1], Nour Arafat[1], Afreen Fatima[1] and
Mohammad RN Avanaki[1,3]

[1]Department of Biomedical Engineering, College of Engineering, Wayne State University, Detroit, MI, USA. [2]School of Health and Related Research, University of Sheffield, Sheffield, UK. [3]Department of Dermatology, Wayne State University, Detroit, MI, USA.

ABSTRACT: Alzheimer disease is the most common form of dementia, affecting more than 5 million people in the United States. During the progression of Alzheimer disease, a particular protein begins to accumulate in the brain and also in extensions of the brain, ie, the retina. This protein, amyloid-β (Aβ), exhibits fluorescent properties. The purpose of this research article is to explore the implications of designing a fluorescent imaging system able to detect Aβ proteins in the retina. We designed and implemented a fluorescent imaging system with a range of applications that can be reconfigured on a fluorophore to fluorophore basis and tested its feasibility and capabilities using Cy5 and CRANAD-2 imaging probes. The results indicate a promising potential for the imaging system to be used to study the Aβ biomarker. A performance evaluation involving ex vivo and in vivo experiments is planned for future study.

KEYWORDS: Fluorescence imaging, Cy5, CRANAD-2, amyloid-β, Alzheimer disease, early diagnosis, instrumentation

Introduction

In the United States, there are currently 5 million people affected by Alzheimer disease (AD). Alzheimer disease is a common form of dementia that severely affects a person's cognitive processes, most notably, significant memory loss. It is one of the top 10 causes of death that cannot be prevented, cured, or slowed.[1] One of the largest obstacles in developing a treatment for AD is the inability to detect it in its early stages. Early treatment of AD would play a fundamental role in preventing the memory loss associated with AD, helping to reduce the devastating emotional and psychological effects of the disease. Alzheimer disease typically goes undetected for years, at which point significant anatomical and physiological changes have occurred in the brain structures—including atrophy and toxic plaque buildup, causing a steady decline in mental capabilities and memory processes before diagnosis.[2] Current detection methods for AD are both expensive and ineffective in catching the disease in its early stages. Early detection of AD is limited when using structural magnetic resonance imaging (MRI), as the scans are largely used to identify atrophy in brain structures. The atrophy of the brain is a symptom of neurodegeneration accompanying AD; however, neurodegeneration is not limited to AD. Neurodegeneration also occurs in Parkinson disease and other forms of dementia. Furthermore, the identification of AD through an MRI tends to occur in later stages of the disease, making it an ineffective method for early detection of AD.[3] In positron emission tomography scans, the person is subjected to radiation thereby limiting the number of images that can be collected in one period of time. Positron emission tomographic images do not tend to be used for high-resolution purposes or structural imaging.[4] In addition, due to its high cost and use of radioactive isotopes, the technology is difficult to employ as an early-onset screening tool for every individual.[5,6] The most promising biomarkers to identify AD are amyloid-β (Aβ) proteins.[7,8] These proteins reveal a significant structure that is key to understand the prognosis of AD. The Aβ proteins have been found in cerebrospinal fluid (CSF). When collected in CSF, it is possible to characterize the amount of amino acids in the Aβ and to determine the extent of plaque development. Although spinal taps give detailed information about the status of AD, it is an incredibly painful and invasive procedure. It would be near impossible to perform this method multiple times and is often only administered in the late stages of AD.[9] Several studies involving the development of Aβ in patients with AD focus on the nervous system, ie, the brain or the spinal cord.[3,4,8–11] The retina, as an extension of the nervous system, has proven to be a window into the pathologies of the brain. The development of Aβ in the brain is typically mirrored in the retina, especially in the primary visual cortex.[12] This is a significant point of interest for the development of early detection methods for AD.[10] Because Aβ proteins have a fluorescent nature, they can be bound to imaging probes to allow for their visualization with the use of fluorescent imaging (FLI) technologies.

The FLI is an optical imaging technique that provides high-resolution images of the fluorescent nature of certain
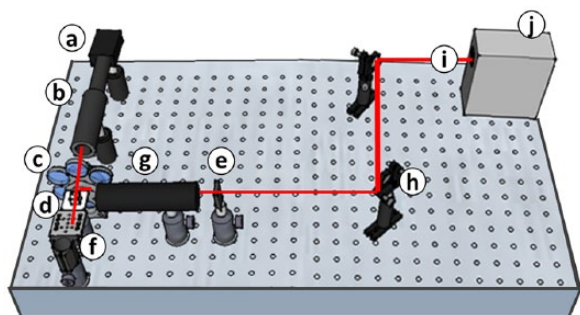
Figure 1. Experimental setup of the fluorescent imaging: (a) camera, (b) imaging lens, (c) emission filter, (d) 1-inch beam splitter, (e) iris, (f) sample holder, (g) beam expander, (h) mirrors, (i) laser pathway, and (j) tunable laser.

molecules, ie, fluorophores. Fluorescence is characterized as the absorption and subsequent radiation of light by a specimen. Exogenous fluorophores, ie, imaging probes, bind to a specific molecule and allow for a clearer fluorescent image. Considering the development of Aβ on the retina, their small size in soluble form, and their ability to bind to fluorescent probes, obtaining fluorescent images of these proteins provides a promising method toward early detection of AD. Certainly, the clinical relevance of imaging Aβ for diagnostic purposes has been a topic of increasing interest. In their critical review of using Aβ sequelae in the eye as a diagnostic marker for AD, Shah et al[13] indicate that observations of the lens and retina are the most promising avenues for this purpose. The authors identify fluorescence as an encouraging modality for this identification but highlight the difficulty to distinguish endogenous fluorophores from biomarkers. This indicates the need for a more robust system capable of identifying exogenous and endogenous fluorophores.

Biomarkers, such as CRANAD-2, have been previously used (oral or intravenous administration) due to their affinity to Aβ plaques.[14–18] CRANAD-2 is derived from curcumin, a component of turmeric which has shown to have benefits in reducing Aβ aggregation, as well as other health benefits.[15] The probe shows a significant enhancement of its fluorescent properties when in the presence of amyloid fibrils.[15] Ran et al[16] designed a CRANAD-2 probe specifically as an Aβ plaque marker for near-infrared (NIR) fluorescent imaging. The probe showed a specific affinity to the Aβ plaques, making it an ideal marker for fluorescent imaging.[16] These biomarkers appear to activate in the presence of the plaques, showing measurable fluorescence.[17] Imaging the probes through the retina allows changes to retinal tissue caused by Aβ plaque to be observed, thus decreasing the invasiveness of a diagnosis.[18] In 2010, Karonyo-Hamaoui et al[19] systemically administered curcumin to detect Aβ plaques in live AD-Tg mice and were then able to optically image retinal Aβ plaques in vivo, reporting that these plaques were not detected in non-Tg mice. In the same groundbreaking article, in 2011, Karonyo-Hamaoui et al[19] confirm the presence of retinal Aβ plaques in postmortem eyes of patients

with AD as well as in patients suspected to have had early stages of AD. Further studies indicate that retinal plaques may associate with blood vessels in the superior quadrant and have an amyloid pathology similar to the brain.[5,6,19–21] Moreover, the use of this biomarker extends beyond Aβ as Park et al[22] further explored the use of CRANAD-2 in imaging tau fibrils. In addition, a variety of other probes with an affinity for Aβ have been detailed by Xu et al.[23] These authors suggest the use of probes with a near NIR wavelength emission between 650 and 900 nm to avoid background fluorescence from brain tissue.

In this study, we develop a fluorescent imaging system that can be used as a noninvasive detection method which could be administered frequently and easily in a clinical setting. The system is designed for viewing the development of Aβ plaque on the retina by imaging fluorescent probes with NIR emission spectra. Moreover, as this low-cost optical imaging system is refined, it may have utility in other fields of medicine. Further research is needed to investigate its uses. For this reason, we have designed the imaging setup and validation process to enable the development of similar systems for other scientific areas.

## Materials and Methodology

Experimental system setup

A Xiton Tunable Laser, ranging from 520 to 1024 nm, was used in our experiments as the excitation source. It allows adjustments of the excitation wavelength and the output power of the laser, to efficiently excite the fluorophores. The beam was spatially filtered by means of a standard iris (D12S; Thorlabs, Newton, NJ, USA). A 1-inch beam splitter (BS019; Thorlabs) was used for directing the light toward the sample and to split the beam power. The beam splitter directs the light onto the sample and allows the camera to image the sample in alignment with the beam path. Bandpass filters (FB 720-10 and FB 810-10; Thorlabs) were used as fluorescence emission filters for 710 and 810 nm, respectively. A CMOS Camera with the pixel size of 5.5 μm (GS3-U3-41CNIR-C; Point Grey, Richmond, BC, Canada) was chosen due to its capabilities to detect Aβ fluorescence with a high quantum efficiency at the wavelength range between 450 and 800 nm. A zooming, telocentric lens (VZM 450i; Edmund Optics Inc., Barrington, NJ, USA) with an adjustable zoom from ×1 to ×4 was used as the objective lens on the camera. The working resolution was determined as 5 μm (measured by a 1951 USAF resolution target). Figure 1 depicts the experimental imaging setup.

This system has the potential to be modified for a range of applications and can be reconfigured on a fluorophore to fluorophore basis. There are 2 modifications that have been developed and implemented for future experiments: the incorporation of a beam expander and a motorized emission filter wheel. The ability to magnify the beam is beneficial for imaging the entire retina. Emission filters allow a wavelength of the fluorophore to pass to the camera. However, in some cases, a sample may exhibit more than one fluoresce; since the imaging probe can have 2
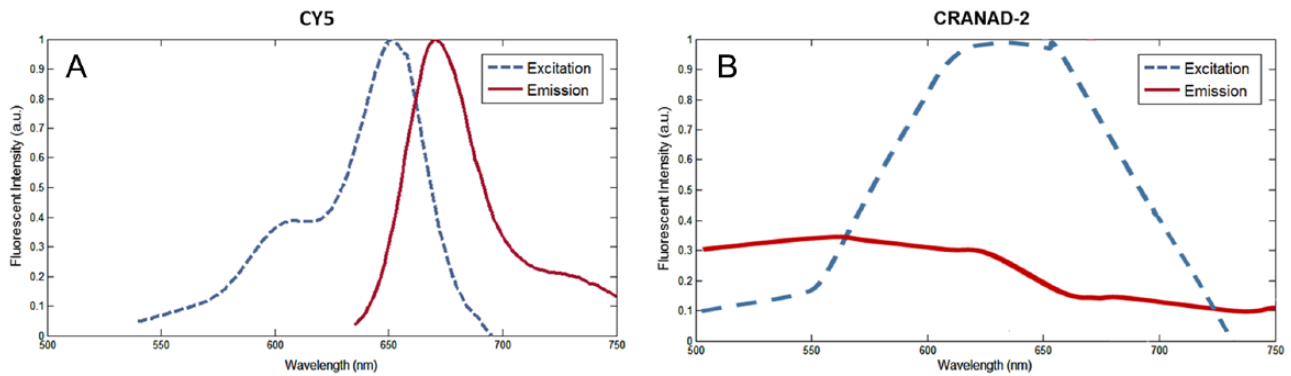
Figure 2. (A) Spectra of Cy5 for fluorescence emission and excitation. Peak wavelength of excitation is at 649 nm, and the peak emission is at 675 nm. (B) Spectra of CRANAD-2 for fluorescence emission and excitation. Peak wavelength of excitation is at 649 nm, and the peak emission is at 525 nm.[16,24]
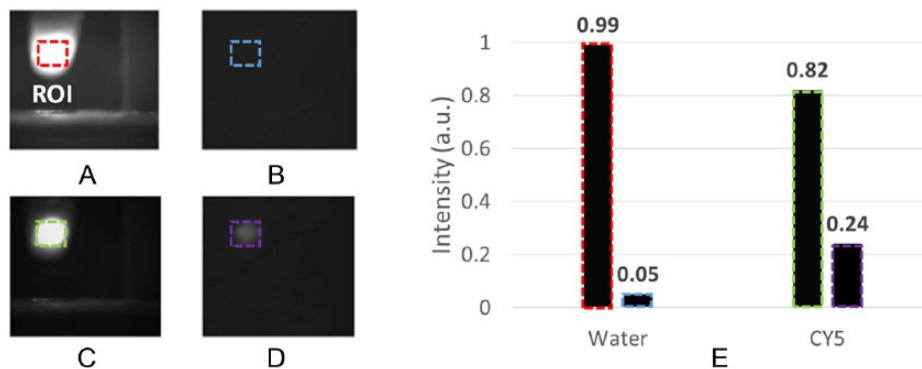
Figure 3. Images of water illuminated with λ-excitation of 649 nm: (A) without emission filter and (B) with 710 nm emission filter. Images of Cy5 illuminated with λ-excitation of 649 nm: (C) without emission filter and (D) with emission 710 nm filter. (E) Averaged intensity of the pixels in the ROI indicated by the boxes in (A).

different emission wavelengths—one when they are bound to their target molecule and another when they are not bound to the target molecule. Capturing an image of each instance is crucial for understanding the sample. The motorized emission filter wheel is used for this purpose. The wheel is programmed with the Arduino to allow for the switches between emission filters.

Experimental system testing

To understand the fluorescent detection capabilities of our imaging system, a series of experiments were performed with Cyanine-5 (Cy5), a well-researched fluorophore. Cy5 is best excited at a wavelength of 649 nm and emits the finest fluorescent response at 675 nm. The full spectra of Cy5 are depicted in Figure 2A. To determine the feasibility of the imaging system in the diagnosis of AD, CRANAD-2 was also tested as an imaging probe. Through this experiment, it can be determined whether this system has the potential to detect Aβ in the retina. A previous study by Ran et al has determined the fluorescence spectra of CRANAD-2, both bound and unbound, to Aβ proteins. The spectra determined for unbound CRANAD-2 are depicted in Figure 2B.[16,24] In accordance with the excitation wavelength of CRANAD-2, the laser was tuned to excite the sample using a 640 nm wavelength. A 710 nm filter would allow for the detection of CRANAD-2 bound to Aβ proteins.

Results and Discussion

Fluorescent detection

The first experiment was to prove that the fluorescent imaging system can detect a fluorescent response from the Cy5 dye. The use of Cy5 as a fluorophore allowed for a series of tests to understand the optical modulation of the system and to determine the best settings for the camera and laser. Two samples were imaged in this experiment: a microcentrifuge tube containing water was used as the control and a microcentrifuge tube containing Cy5 dye (12.5% concentration) was used as the variable. The results of the fluorescent experiment with water are shown in Figure 3A and B. When the water was imaged without an emission filter, the object was seen clearly in the image. However, when imaged with the emission filter, no fluorescent response was detected. The results of the fluorescent experiment with Cy5 also provided the expected results. When the Cy5 was imaged without an emission filter, it was detected clearly by the camera as shown in Figure 3C. In addition, when the Cy5 was imaged with the 710 nm emission filter in place, its fluorescent response was detected, as shown in Figure 3D. To obtain quantitative values, a region of interest of 100 × 100 pixels was measured within each experimental image to determine the intensity value as shown in Figure 3E.
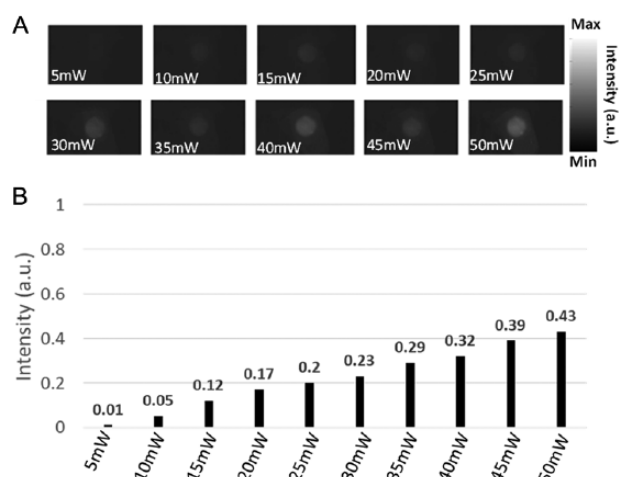
Figure 4. (A) Fluorescent imaging of Cy5 target at different optical excitation powers with a 710 nm emission filter. Colorbar depicts fluorescent intensity (a.u.). (B) Quantitative intensity of images.

This experiment demonstrates the fluorescent detection capabilities of our imaging system.

Optimizing laser optical power

Illuminating the fluorescent sample with the correct excitation wavelength is not the only necessary consideration when using an excitation source. The power of the source also needs to be optimized to have sufficient absorption. For this experiment, a sample of Cy5 was illuminated at 649 nm to match its peak excitation wavelength. The power of the laser was incrementally increased 10 times from 5 to 50 mW. Figure 4 shows the results of the fluorescent imaging of Cy5 target at different optical excitation powers. The results were as expected: the increase in optical power increased the fluorescent signal. To obtain quantitative values, an area of 100×100 pixels was measured within each experimental image to determine the intensity value.

Fluorescent response: agar phantom with Cy5 injected

To determine the capability of the system for imaging the fluorescent response, an experiment was conducted on an agar phantom injected with Cy5. The use of agar as a medium for this experiment allows for both convenience and control over the imaging of the fluorescent material. A 3% agar phantom was created using standard laboratory techniques. Agar and distilled water were mixed and heated to a boil with constant stirring to ensure full incorporation of the powder. The heated mixture was poured into small molds to allow it to cool and solidify. The Cy5 (with 5% concentration) was injected into areas as large as 4×4 mm^2 and into areas as small as 900×900 μm^2 (see Figure 5). A Petri dish containing this medium was held upright to allow for the imaging of the agar phantom with Cy5 injected.

However, the Cy5 in the phantom produced a fluorescent response; a noticeable difference between the variations of the Cy5 c concentrations was not clearly observed.
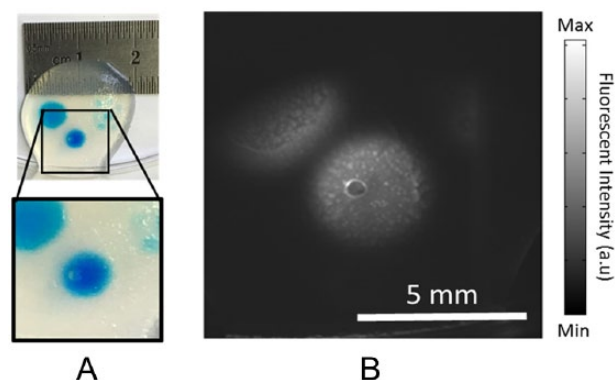
Figure 5. Agar phantom with Cy5 dye–injected areas. (A) Agar phantom with Cy5-injected areas. The square depicts the field of view of our imaging. (B) Florescent image of the phantom.

Fluorescent response: agar phantom with CRANAD-2 particles

Two samples were made for this experiment: a blank agar phantom and an agar phantom with CRANAD-2 particles in it. Figure 6A and B depicts the samples used in this experiment. The fluorescent images of the samples are given in Figure 6C and D. To obtain quantitative values, an area of 100×100 pixels was considered within each experimental image to determine the intensity value. The excitation and emission wavelengths were 649 and 710 nm, respectively.

These results in Figure 6 demonstrated that CRANAD-2 could produce a signal; however, the fluorescent signal of the CRANAD-2 was weak. The weak signal of CRANAD-2 is not entirely unexpected, as there was no binding agent for the dye to bond with. As detailed by Ran et al,[24] when CRANAD-2 is imaged without being bound to an Aβ, it has a lower fluorescent signal strength.

Summary and Future Work

With an intention to develop a system that can identify AD at an early stage, we designed a fluorescent imaging system to image Aβ proteins. The resolution of the imaging system was sufficient to image microstructures as small as 5 μm. The performance of the system was tested using several phantoms. Different laser optical powers were tested. Two dyes were tested including Cy5 and CRANAD-2. CRANAD-2 was the primary contrast agent chosen for its use in diagnosing AD. Cy5 was selected for the similarity in excitation-emission spectra to CRANAD-2 and for its strong fluorescent response which helped to validate our design. The experiment used an agar phantom injected with Cy5 dye at different concentrations and an agar phantom containing CRANAD-2 particles. We demonstrated that the system will be capable of detecting the fluorescent phenomenon of an Aβ protein as we could image CRANAD-2. The system is capable of being used for a wide range of applications and can be modified on a fluorophore to fluorophore basis. In future testing, phantom imaging of Aβ mixed with the CRANAD-2 will be performed to measure the ratio of bound to unbound CRANAD-2 particles and the type of fluorescent signal exhibited. In addition, future experiments
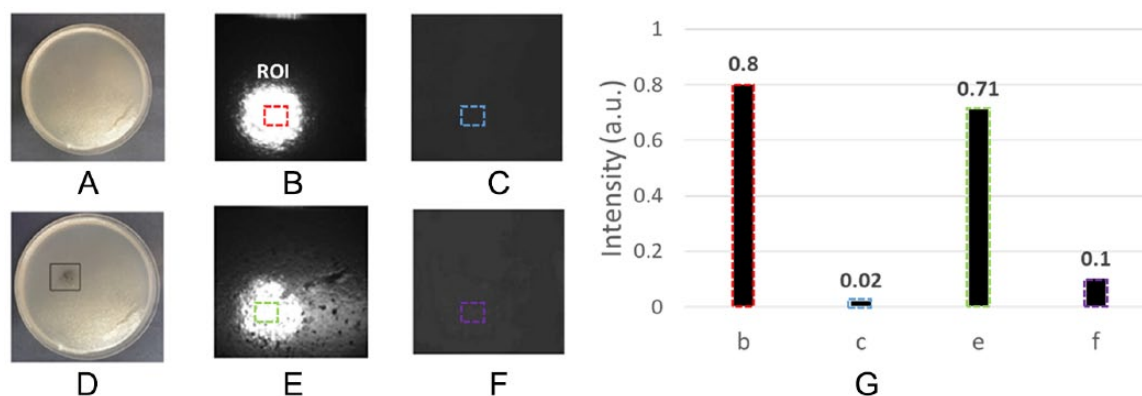
Figure 6. Agar phantom constructed for CRANAD-2 testing. (A) A blank agar phantom (B) illuminated with 649 nm with no emission filter and (C) with 710 nm emission filter. (D) A phantom that has CRANAD-2 particles injected in it (E) illuminated with 649 nm with no emission filter, and (F) with 710 nm emission filter. (G) Averaged intensity of the pixels in the ROI indicated by the boxes in (A).

for in vivo retina imaging will be performed to determine whether CRANAD-2 and Aβ can be seen in an AD model.

This research provides validation for a simplified imaging system for the detection of Aβ proteins using fluorescence imaging techniques. In addition, the development of a functioning imaging system with the capabilities of probe to probe variation is presented. Acknowledgements of the limitations of this study include those that result from the experimental design. The exploration of similar and alternative biomarkers for Aβ is warranted to determine the most feasible options for diagnosis using fluorescent imaging. Optimization of the imaging system will increase the robustness of its capabilities. Laser safety will be provided by an optimum mechanical design of the device housing in which a beam dump is well-integrated.

Future work based on this design would involve in vivo imaging to validate its diagnostic potential. This could involve using such a system in conjunction with optical coherence tomography (OCT) to enhance its diagnostic capability.[25,26] This combined system would allow for a noninvasive means to potentially diagnose AD with higher confidence, early in the disease's progression. The fluorescence imaging system and components would be modified and compacted to create a system with which a patient could simply peer into an opening to image their retina. Such a machine would be designed and used in a manner similar to the OCT machines currently being used in ophthalmology. Once developed, this system could easily be implemented into an optometry practice to improve diagnostic procedures and outpatient services.

REFERENCES

1. Alzheimer's Association. *Latest Alzheimer's Facts and Figures*. Chicago, IL: Alzheimer's Association; 2013.
2. Kumar A, Singh A, Ekavali. A review on Alzheimer's disease pathophysiology and its management: an update. *Pharmacol Rep*. 2015;67:195–203.
3. Kirbas S, Turkyilmaz K, Anlar O, Tufekci A, Durmus M. Retinal nerve fiber layer thickness in patients with Alzheimer disease. *J Neuroophthalmol*. 2013;33:58–61.
4. Lewczuk P, Mroczko B, Fagan A, Kornhuber J. Biomarkers of Alzheimer's disease and mild cognitive impairment: a current perspective. *Adv Med Sci*. 2015;60:76–82.
5. Hart NJ, Koronyo Y, Black KL, Koronyo-Hamaoui M. Ocular indicators of Alzheimer's: exploring disease in the retina. *Acta Neuropathol*. 2016;132:767–787.
6. Doustar J, Torbati T, Black KL, Koronyo Y, Koronyo-Hamaou M. Optical coherence tomography in Alzheimer's disease and other neurodegenerative diseases. *Front Neurol*. 2017;8:701.
7. Blennow K. Biomarkers in Alzheimer's disease drug development. *Nat Med*. 2010;16:1218–1222.
8. Goldman B. *Scientists Reveal How Beta-amyloid May Cause Alzheimer's*. Stanford, CA: News Center, Stanford University; 2013.
9. Rowe CC, Villemagne VL. Amyloid imaging with PET in early Alzheimer disease diagnosis. *Med Clin North Am*. 2013;97:377–398.
10. Ahmed M, Davis J, Aucoin D, et al. Structural conversion of neurotoxic amyloid-beta(1-42) oligomers to fibrils. *Nat Struct Mol Biol*. 2010;17:561–567.
11. Serrano-Pozo A, Mielke ML, Muzitansky A, et al. Stable size distribution of amyloid plaques over the course of Alzheimer disease. *J Neuropathol Exp Neurol*. 2012;71:694–701.
12. Koronyo Y, Biggs D, Barron E, et al. Retinal amyloid pathology and proof-of-concept imaging trial in Alzheimer's disease. *JCI Insight*. 2017;2:93621.
13. Shah TM, Gupta SM, Chatterjee P, Campbell M, Martins RN. Beta-amyloid sequelae in the eye: a critical review on its diagnostic significance and clinical relevance in Alzheimer's disease. *Mol Psychiatry*. 2017;22:353–363.
14. Shoup T, Elmaleh D, Carter E, et al. Synthesis and biodistribution of F-18 labeled scyllo-inositol derivatives as potential probes for detecting amyloid beta oligomers. *J Nucl Med*. 2009;50:1935–1935.
15. Staderini M, Martín MA, Bolognesi ML, Menéndez JC. Imaging of β-amyloid plaques by near infrared fluorescent tracers: a new frontier for chemical neuroscience. *Chem Soc Rev*. 2015;44:1807–1819.
16. Ran C, Xu X, Raymond SB, et al. Design, synthesis, and testing of difluoroboron-derivatized curcumins as near-infrared probes for in vivo detection of amyloid-β deposits. *J Am Chem Soc*. 2009;131:15257–15261.
17. Xu M, Ren W, Tang X, Hu Y, Zhang H. Advances in development of fluorescent probes for detecting amyloid-β aggregates. *Acta Pharmacol Sin*. 2016;37:719–730.
18. Koronyo Y, Salumbides BC, Black KL, Koronyo-Hamaoui M. Alzheimer's disease in the retina: Imaging retinal aβ plaques for early diagnosis and therapy assessment. *Neurodegener Dis*. 2012;10:285–293.
19. Koronyo-Hamaoui M, Koronyo Y, Ljubimov AV, et al. Identification of amyloid plaques in retinas from Alzheimer's patients and noninvasive in vivo optical imaging of retinal plaques in a mouse model. *NeuroImage*. 2011;54:S204–S217.
20. La Morgia C, Ross-Cisneros FN, Koronyo Y, et al. Melanopsin retinal ganglion cell loss in Alzheimer disease. *Ann Neurol*. 2016;79:90–109.
21. Tsai Y, Lu B, Ljubimov AV, et al. Ocular changes in TgF344-AD rat model of Alzheimer's disease. *Invest Ophthalmol Vis Sci*. 2014;55:523–534.
22. Park KS, Seo Y, Kim MK, et al. A curcumin-based molecular probe for near-infrared fluorescence imaging of tau fibrils in Alzheimer's disease. *Org Biomol Chem*. 2015;13:11194–11199.
23. Xu M-M, Ren WM, Tang XC, Hu YH, Zhang HY. Advances in development of fluorescent probes for detecting amyloid-β aggregates. *Acta Pharmacol Sin*. 2016;37:719–730.
24. Ran C, Zhao W, Moir RD, Moore A. Non-conjugated small molecule FRET for differentiating monomers from higher molecular weight amyloid beta species. *PLoS ONE*. 2011;6:e19362.
25. Adabi S, Turani Z, Fatemizadeh E, Clayton A, Nasiriavanaki M. Optical coherence tomography technology and quality improvement methods for optical coherence tomography images of skin: a short review. *Biomed Eng Comput Biol*. 2017;8:1179597217713475.
26. Adabi S, Fotouhi A, Xu Q, et al. An overview of methods to mitigate artifacts in optical coherence tomography imaging of the skin. *Skin Res Technol*. 2018;24:265–273.